Radiation Transport Models in Space: from Supernovae to Cells

Tony C. Slaba

NASA Langley Research Center, USA

Durability, Damage Tolerance, and Reliability Branch

MaThRad 2nd Clinical Workshop

November 8, 2023

Outline

- Space radiation overview – what, why, how?
- Radiation transport
  - Cosmic ray propagation in the galaxy (Fokker-Planck)
  - Radiation transport through shielding (Boltzmann)
  - Microscopic scale electron transport (Monte Carlo simulation)
- NASA cancer risk model projections for exploration missions
- Summary

Space Radiation Overview

- **What** → Space radiation is identified by NASA as one of the five hazards of human spaceflight

https://www.nasa.gov/organizations/ochmo/human-spaceflight-hazards/

Space Radiation Overview

- **<u>Why</u>** → Space radiation is qualitatively different than any form of radiation on Earth

Radiation sources on Earth

- Mainly gammas and x-rays
  - Waste, accidents, weapons
  - Occupational (medical and nuclear industries)
  - Natural terrestrial sources (e.g. radon)
- Epidemiological data exist to guide risk assessment and set conservative protection limits
- Protection strategies guided by
  - Limiting exposure time
  - Increasing distance from source
  - Shielding

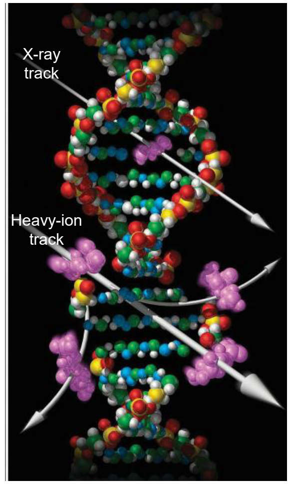

https://www.nasa.gov/stem-content/modeling-radiation-damaged-dna/

humanresearchroadmap.nasa.gov/evidence/reports/Carcinogenesis.pdf

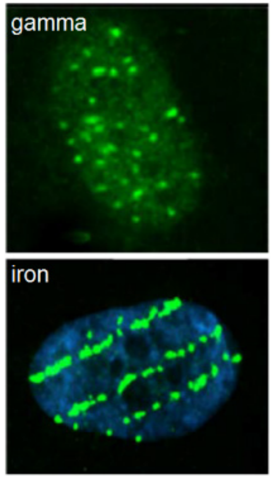

Space Radiation

- Highly energetic particle radiation
  - Everything on the periodic table of elements
  - Able to penetrate shielding and tissue
- No direct means of assessing health risks
  - Limited human data
  - Lack of mechanistic knowledge
- Earth protection strategies do not work
  - Exposure time controlled by mission requirements
  - Space radiation is ubiquitous
  - Shielding strategies are limited

Space Radiation Overview

- **<u>How</u>** → Space radiation exposures and risks are estimated using integrated models and data

Space radiation environment

nasa.gov/sites/default/files/14-271.jpg

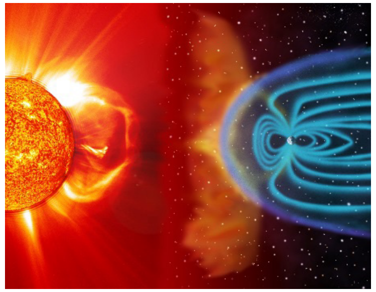

Intravehicular radiation field

Simonsen, Slaba, Guida, Rusek, *Plos Bio* **18**: e3000669; 2020.

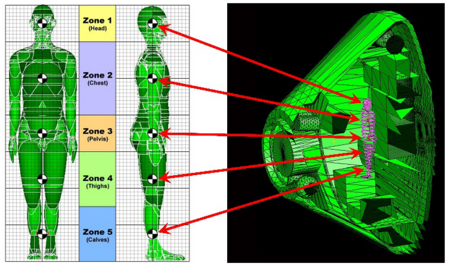

Health risk projections

Simonsen, Slaba, Guida, Rusek, *Plos Bio* **18**: e3000669; 2020.

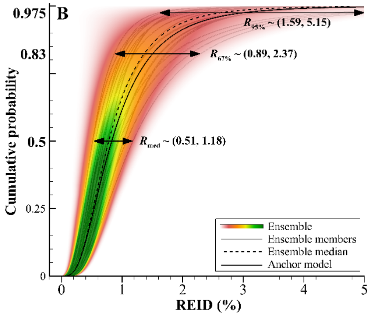

- Models propagate cosmic rays outside the galaxy to near Earth
- Guided by available measurements

- Transport codes used to assess intravehicular radiation field
- Guided by inter-code comparisons and available measurements

- Risks evaluated probabilistically to account for significant uncertainties
- Guided by epidemiological data and radiobiology experiments

Space Radiation Overview

- **<u>How</u>** → Space radiation exposures and risks are estimated using integrated models and data

Space radiation environment

nasa.gov/sites/default/files/14-271.jpg

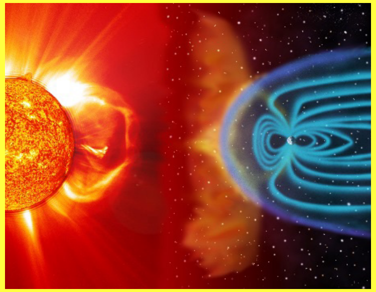

→

Intravehicular radiation field

Simonsen, Slaba, Guida, Rusek, *Plos Bio* **18**: e3000669; 2020.

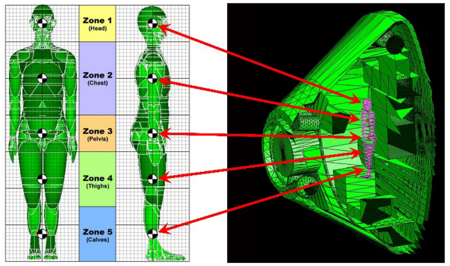

→

Health risk projections

Simonsen, Slaba, Guida, Rusek, *Plos Bio* **18**: e3000669; 2020.

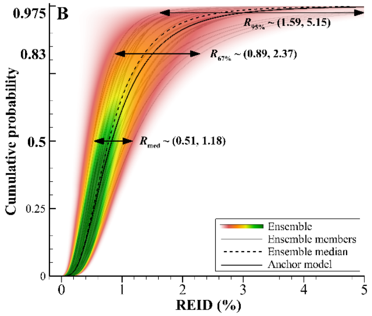

Galactic Cosmic Rays

- Galactic cosmic rays (GCR) are the main radiation hazard for long duration exploration missions
  - Broad spectrum of particle types
  - Ion velocities approach the speed of light (penetrating)
  - Fluctuate between solar minimum/maximum on 11-year cycle
  - Low dose-rate

Relative abundance of elements in the 1977 solar minimum GCR environment, normalized to Ne

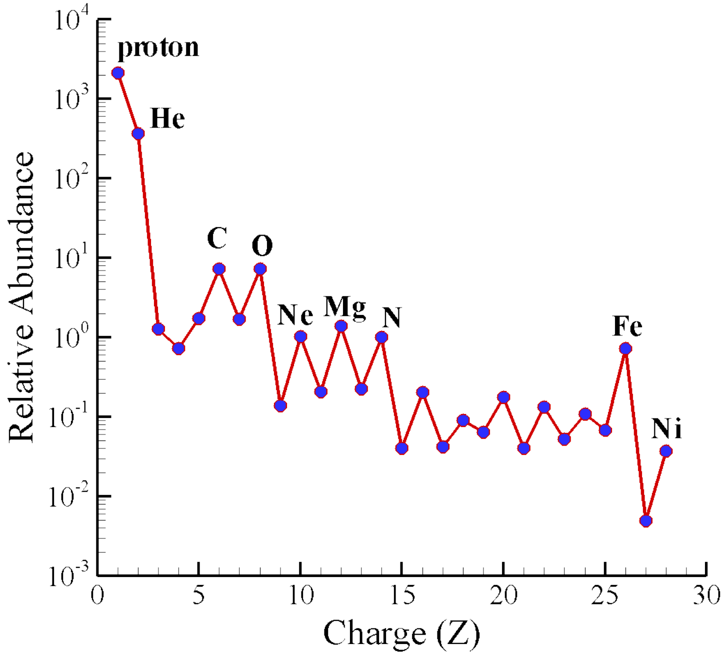

GCR proton flux (April 13 – May 9, 2017).

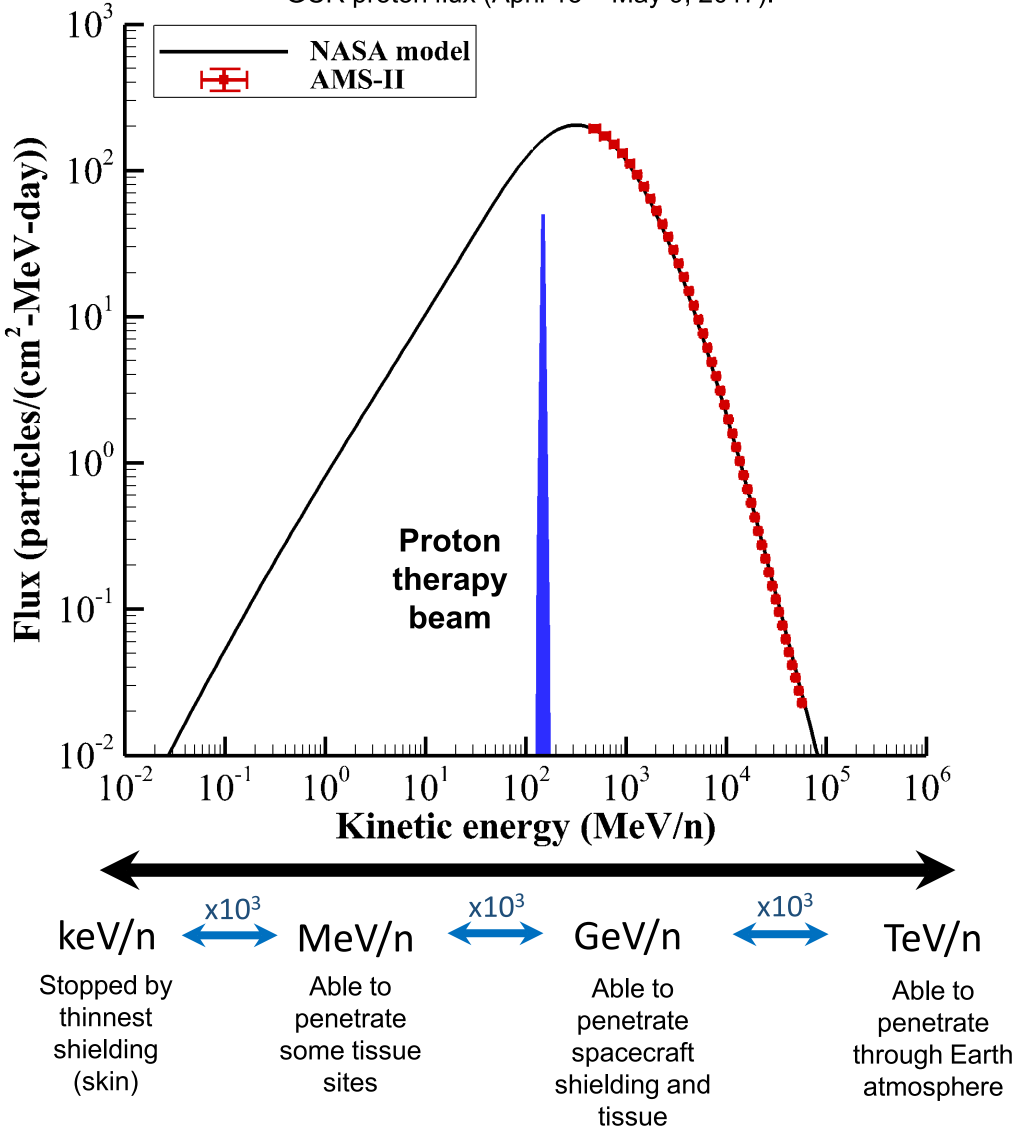

GCR Models

- The NASA model for calculating the GCR field near Earth is the Badhwar-O'Neill (BON) model
  - Originally developed in the early 1990s
  - Assumes steady-state, radially symmetric transport through the heliosphere
  - Transport cosmic ray spectrum at edge of heliosphere to 1 astronomical unit
  - Utilizes numerical solution to the Fokker-Planck equation

$$\frac{1}{r^2}\frac{\partial}{\partial r}\left(r^2 V_{sw} U\right) - \left[\frac{1}{3r^2}\frac{\partial}{\partial r}\left(r^2 V_{sw}\right)\right]\left[\frac{\partial}{\partial T}\left(TU\,\frac{T+2m}{T+m}\right)\right] - \frac{1}{r^2}\frac{\partial}{\partial r}\left(r^2 \kappa \frac{\partial U}{\partial r}\right) = 0$$

$U(r,T)$	Omnidirectional particle density distribution
r	distance from the Sun
T	ion kinetic energy (MeV/n)
κ	diffusion coefficient
V_{sw}	solar wind speed
m	ion rest mass

Further reading

- Detailed derivation of transport equation
  - Mertens, Meier, Brown, Norman, Xu, *Space Weather* **11**: 603-605; 2013.
- Description of Crank-Nicholson numerical solution
  - Slaba, Whitman, NASA/TP-2019-220419; 2019.
- Current version – BON2020
  - Slaba, Whitman, *Space Weather* **18**: e2020SW002456; 2020.

GCR Model Results

- **BON2020 model is accurate and computationally efficient**

	Average absolute model error against all measurements (N=27,646)
BON2014	12%
BON2020	5%

Slaba, Whitman, *Space Weather* **18**: e2020SW002456; 2020.

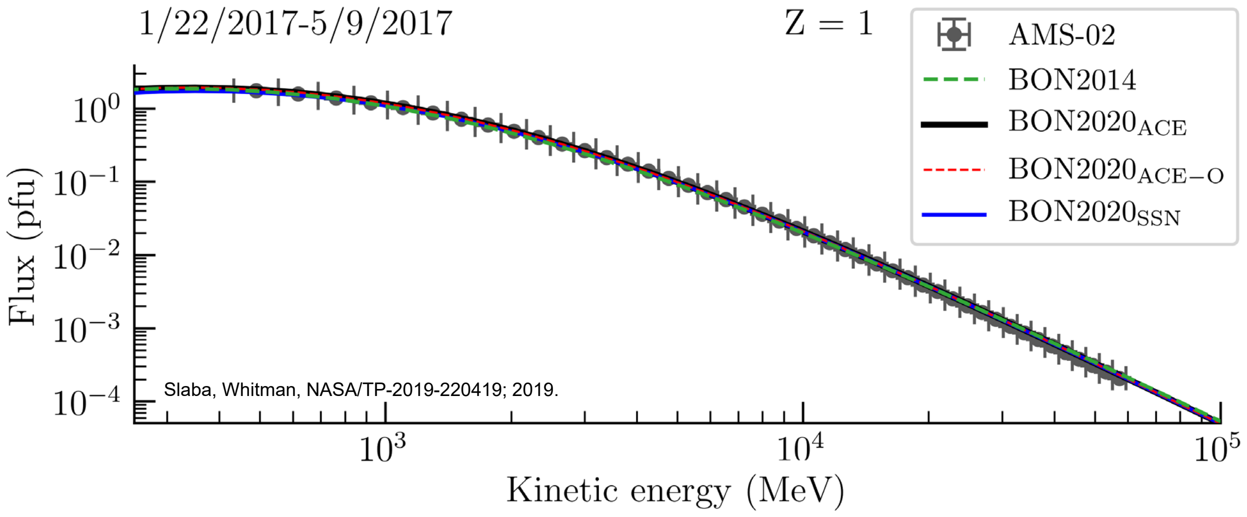

Comparison of model Z = 1 flux to AMS-02 measurements integrated over 1/22/2017-5/9/2017. For this plot, particle flux units (pfu) are defined as particles/(cm^2-MeV-day).

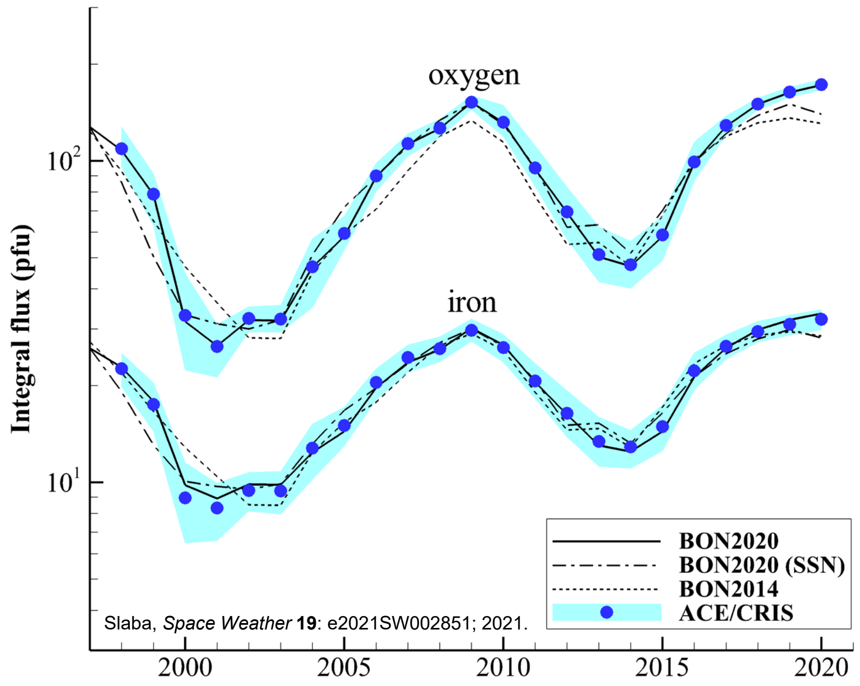

Comparison of BON2020 model calculations to ACE/CRIS measurements of oxygen and iron integral flux. For this plot, particle flux units (pfu) are defined as particles/(cm^2-day).

SSN – Sunspot number
AMS-02 – Alpha Magnetic Spectrometer 02
ACE/CRIS - Advanced Composition Explorer/Cosmic Ray Isotope Spectrometer

Other GCR Models

- Many other GCR models and solution methodologies exist
  - Applications of interest vary
  - Wide range of model fidelities and computational costs
  - Recent summary and comparison: Liu, Guo, Wang, Slaba, *ApJ*, submitted; 2023.

Empirical → Full-scale simulation

- ❖ **CREME2009** (Cosmic Ray Effects on MicroElectronics)
  - Based on semi-empirical ISO 15390 model with low energy corrections of interest to electronics effects

    Adams, Barghouty, Mendenhall, *IEEE Trans. Nuc. Sci.* **59**: 3141; 2012.
- ❖ **DLR2013** (German Aerospace Center)
  - Based on semi-empirical ISO 15390 model with simplified time-dependent solar modulation

    Matthia, Berger, Mrigakshi, Reitz, *Adv. Space Res.* **51**: 329; 2013.
- ❖ **SINP2016** (Skobeltsyn Institute of Nuclear Physics)
  - Based on semi-empirical ISO 15390 model with radial corrections and SSN time lag

    Kuznetsov, Popova, Panasyuk, *JGR Space Physics* **122**: 1463-1472; 2016.
- ❖ **HelMod** (Heliospheric Modulation)
  - Monte Carlo simulation to solve a set of stochastic differential equations accounting for heliospheric radius and latitude

    Boschini, Della Torre, Gervasi, La Vacca, Rancoita, *Adv. Space Res.* **64**: 2459; 2019.
- ❖ **SDEMMA** (Space-Dependent Energetic cosmic ray Modulation using MAgnetic spectrometer)
  - Solves a set of stochastic differential equations accounting for heliospheric radius, latitude, and longitude

    Chen, Xu, Song, Huo, Luo, *Space Weather* **21**: e2022SW003285; 2023.

SSN – Sunspot number

ISO - International Organization for Standardization

Space Radiation Overview

- **How** → Space radiation exposures and risks are estimated using integrated models and data

Space radiation environment

nasa.gov/sites/default/files/14-271.jpg

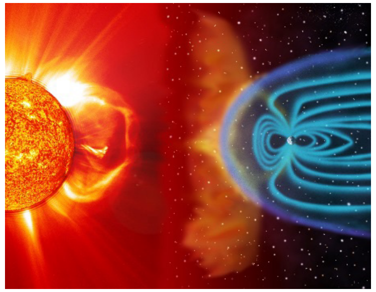

Intravehicular radiation field

Simonsen, Slaba, Guida, Rusek, *Plos Bio* **18**: e3000669; 2020.

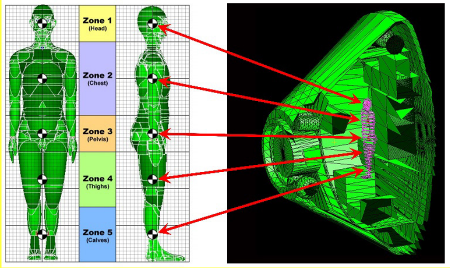

Health risk projections

Simonsen, Slaba, Guida, Rusek, *Plos Bio* **18**: e3000669; 2020.

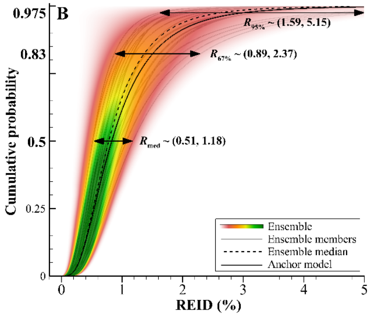

Radiation Transport

- Overall problem description from a NASA perspective
  - Boundary condition is the free space GCR environment
  - Includes particles between Z=1 and Z=28 with energies spanning many orders of magnitude
  - Primary GCR ions interact with shielding and produce secondary particles over broad energies and angles
  - Need to ***accurately and efficiently*** calculate the radiation environment (GCR+secondaries) behind shielding
    - Vehicle/habitat shielding, atmosphere (Earth and Mars), terrestrial soil (moon and Mars)

Further reading

- Wilson et al. publications on this topic too numerous to list here
- General overviews:
  - Wilson, Townsend, Schimmerling, Khandelwal, Khan, Nealy, Cucinotta, Simonsen, Shinn, Norbury, NASA RP-1257; 1991.
  - Wilson, Miller, Konradi, Cucinotta, NASA CP 3360; 1993.
- Most recent NASA model:
  - Werneth, de Wet, Townsend, Maung, Norbury, Slaba, Norman, Blattnig, Ford, *NIM B* **502**: 118-135; 2021.
  - Slaba, Wilson, Werneth, Whitman, *Life Sci. Space Res.* **27**: 2020; 6-18.

Transport Model Development Timeline

- NASA has been developing deterministic transport and nuclear physics models for many decades

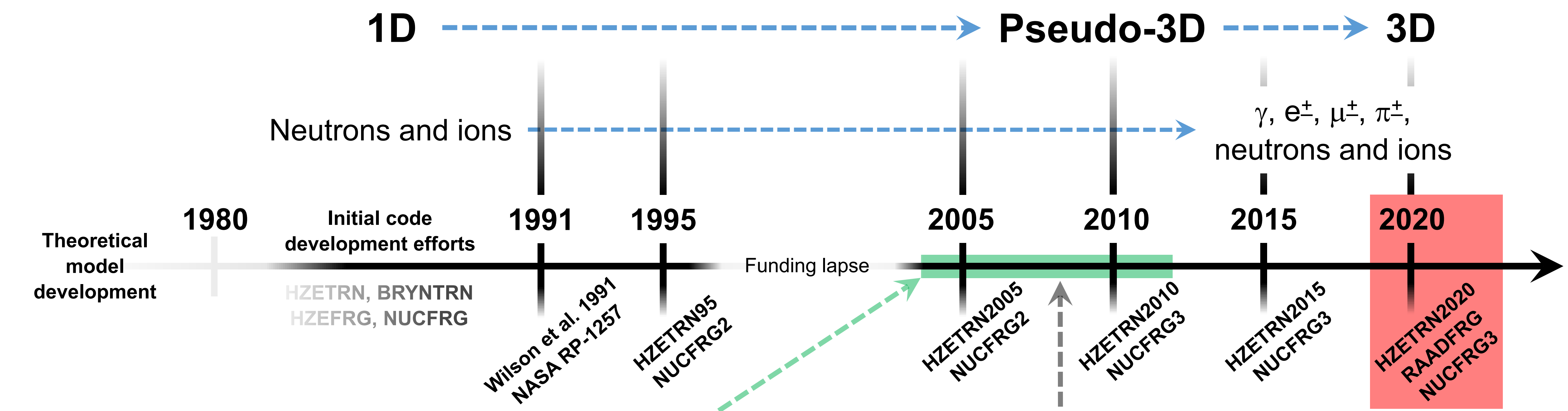

- (GRNTRN) Green's function solutions developed for beam and space boundary conditions
- (CEPTRN) Coupled e± and γ transport code accounting for e⁻ multiple scattering in single layers

https://oltaris.nasa.gov

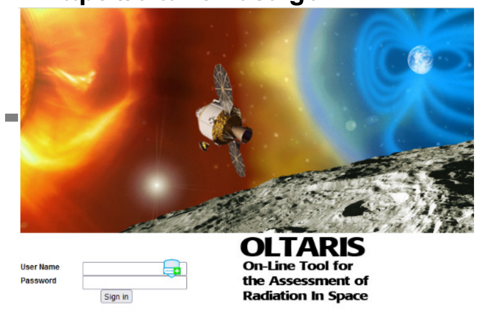

1D – One dimensional
3D – Three dimensional
GRNTRN – Green's function transport

HZETRN/BRYNTRN – NASA deterministic transport codes
HZEFRG/NUCFRG – NASA nuclear fragmentation models
RAADFRG – Most recent NASA nuclear fragmentation model

Boltzmann Transport Equation

- The Boltzmann transport equation within the continuous slowing down approximation may be written as

$$\mathbf{B}[\phi_j(\boldsymbol{x},\boldsymbol{\Omega},E)] = \sum_k \int_E^\infty \int_{4\pi} \sigma_{jk}(E,E',\boldsymbol{\Omega},\boldsymbol{\Omega}')\phi_k(\boldsymbol{x},\boldsymbol{\Omega}',E')\,d\boldsymbol{\Omega}'\,dE' - \sigma_j(E)\phi_j(\boldsymbol{x},\boldsymbol{\Omega},E)$$

where the operator, **B**, is defined as

$$\mathbf{B}[\phi_j(\boldsymbol{x},\boldsymbol{\Omega},E)] \equiv \boldsymbol{\Omega} \bullet \nabla\phi_j(\boldsymbol{x},\boldsymbol{\Omega},E) - \frac{1}{A_j}\frac{\partial}{\partial E}\left[S_j(E)\phi_j(\boldsymbol{x},\boldsymbol{\Omega},E)\right]$$

Boltzmann Transport Equation

- The Boltzmann transport equation within the continuous slowing down approximation may be written as

$$\mathbf{B}[\phi_j(\boldsymbol{x},\boldsymbol{\Omega},E)] = \sum_k \int_E^\infty \int_{4\pi} \sigma_{jk}(E,E',\boldsymbol{\Omega},\boldsymbol{\Omega}')\phi_k(\boldsymbol{x},\boldsymbol{\Omega}',E')\,d\boldsymbol{\Omega}'dE' - \sigma_j(E)\phi_j(\boldsymbol{x},\boldsymbol{\Omega},E)$$

where the operator, **B**, is defined as

$$\mathbf{B}[\phi_j(\boldsymbol{x},\boldsymbol{\Omega},E)] \equiv \boldsymbol{\Omega}\bullet\nabla\phi_j(\boldsymbol{x},\boldsymbol{\Omega},E) - \frac{1}{A_j}\frac{\partial}{\partial E}\left[S_j(E)\phi_j(\boldsymbol{x},\boldsymbol{\Omega},E)\right]$$

$\phi_j(\boldsymbol{x},\boldsymbol{\Omega},E)$ { Flux/fluence of type j particles at position ***x*** moving in the direction **Ω** with kinetic energy, E

Boltzmann Transport Equation

- The Boltzmann transport equation within the continuous slowing down approximation may be written as

$$\mathbf{B}[\phi_j(\boldsymbol{x},\boldsymbol{\Omega},E)] = \sum_k \int_E^\infty \int_{4\pi} \sigma_{jk}(E,E',\boldsymbol{\Omega},\boldsymbol{\Omega}')\phi_k(\boldsymbol{x},\boldsymbol{\Omega}',E')\,d\boldsymbol{\Omega}'dE' - \sigma_j(E)\phi_j(\boldsymbol{x},\boldsymbol{\Omega},E)$$

where the operator, **B**, is defined as

$$\mathbf{B}[\phi_j(\boldsymbol{x},\boldsymbol{\Omega},E)] \equiv \boldsymbol{\Omega} \bullet \nabla \phi_j(\boldsymbol{x},\boldsymbol{\Omega},E) - \frac{1}{A_j}\frac{\partial}{\partial E}\left[S_j(E)\phi_j(\boldsymbol{x},\boldsymbol{\Omega},E)\right]$$

$\phi_j(\boldsymbol{x},\boldsymbol{\Omega},E)$ { Flux/fluence of type j particles at position ***x*** moving in the direction **Ω** with kinetic energy, E

$S_j(E)$ { Stopping power of type j ions at with kinetic energy, E

Boltzmann Transport Equation

- The Boltzmann transport equation within the continuous slowing down approximation may be written as

$$\mathbf{B}[\phi_j(\boldsymbol{x},\boldsymbol{\Omega},E)] = \sum_k \int_E^\infty \int_{4\pi} \sigma_{jk}(E,E',\boldsymbol{\Omega},\boldsymbol{\Omega}')\phi_k(\boldsymbol{x},\boldsymbol{\Omega}',E')\,d\boldsymbol{\Omega}'dE' - \sigma_j(E)\phi_j(\boldsymbol{x},\boldsymbol{\Omega},E)$$

where the operator, **B**, is defined as

$$\mathbf{B}[\phi_j(\boldsymbol{x},\boldsymbol{\Omega},E)] \equiv \boldsymbol{\Omega}\bullet\nabla\phi_j(\boldsymbol{x},\boldsymbol{\Omega},E) - \frac{1}{A_j}\frac{\partial}{\partial E}\left[S_j(E)\phi_j(\boldsymbol{x},\boldsymbol{\Omega},E)\right]$$

$\phi_j(\boldsymbol{x},\boldsymbol{\Omega},E)$ { Flux/fluence of type j particles at position ***x*** moving in the direction **Ω** with kinetic energy, E

$\sigma_j(E)$ { Total nuclear cross section for type j particles with kinetic energy, E

$S_j(E)$ { Stopping power of type j ions at with kinetic energy, E

Boltzmann Transport Equation

- The Boltzmann transport equation within the continuous slowing down approximation may be written as

$$\mathbf{B}[\phi_j(\boldsymbol{x},\boldsymbol{\Omega},E)] = \sum_k \int_E^\infty \int_{4\pi} \sigma_{jk}(E,E',\boldsymbol{\Omega},\boldsymbol{\Omega}')\phi_k(\boldsymbol{x},\boldsymbol{\Omega}',E')\,d\boldsymbol{\Omega}'dE' - \sigma_j(E)\phi_j(\boldsymbol{x},\boldsymbol{\Omega},E)$$

where the operator, **B**, is defined as

$$\mathbf{B}[\phi_j(\boldsymbol{x},\boldsymbol{\Omega},E)] \equiv \boldsymbol{\Omega}\bullet\nabla\phi_j(\boldsymbol{x},\boldsymbol{\Omega},E) - \frac{1}{A_j}\frac{\partial}{\partial E}\left[S_j(E)\phi_j(\boldsymbol{x},\boldsymbol{\Omega},E)\right]$$

$\phi_j(\boldsymbol{x},\boldsymbol{\Omega},E)$ { Flux/fluence of type j particles at position ***x*** moving in the direction **Ω** with kinetic energy, E

$S_j(E)$ { Stopping power of type j ions at with kinetic energy, E

$\sigma_j(E)$ { Total nuclear cross section for type j particles with kinetic energy, E

$\sigma_{jk}(E,E',\boldsymbol{\Omega},\boldsymbol{\Omega}')$ { Double-differential cross section for all interactions in which type j particles (**Ω**,E) are produced by type k particles (**Ω**',E')

Solution Methodology

- Solution methodology based on perturbation theory
  - Solve simple equation with dominant physical terms
  - Substitute simple solution back into Boltzmann equation
  - Repeat or approximate remainder terms
  - Fast and accurate stepping procedure with linear spline expansion of integrals when necessary
  - Solutions do not use finite difference or finite element methods

- 1D and 3D solutions
  - Both used in specific applications depending on fidelity and accuracy requirements

Neutron production energy spectrum for a 1 GeV proton incident on an aluminum target.

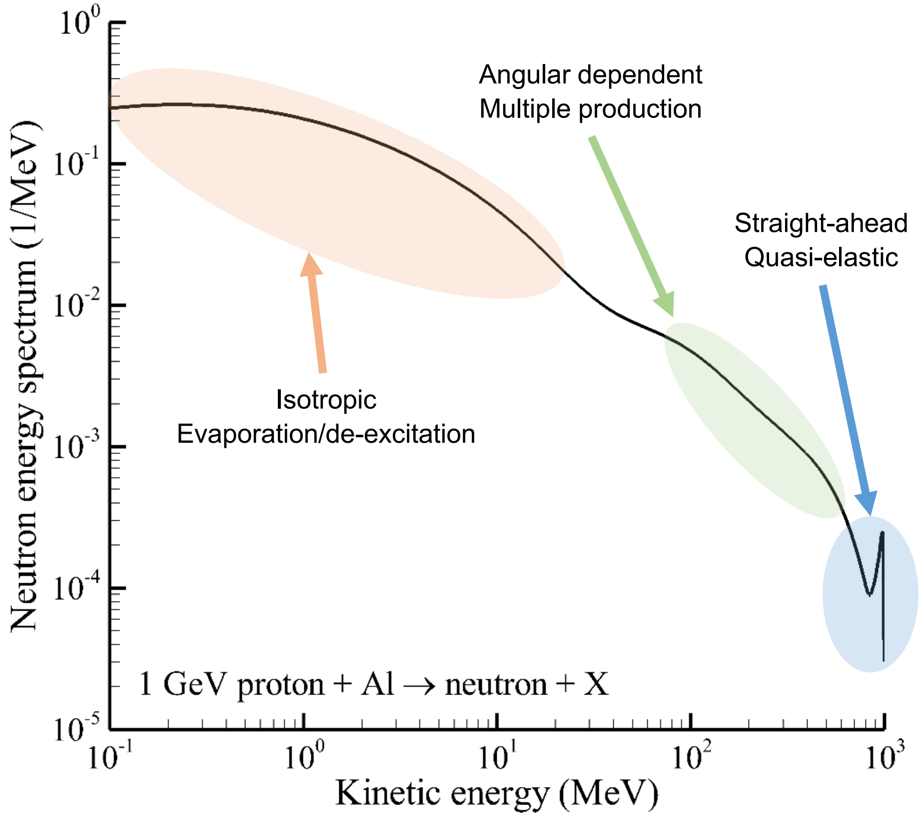

Verification

- **HZETRN2020 able to reproduce Monte Carlo simulations if same cross sections are used**

Geometry used for comparison between 3DHZETRN and Monte Carlo simulation.

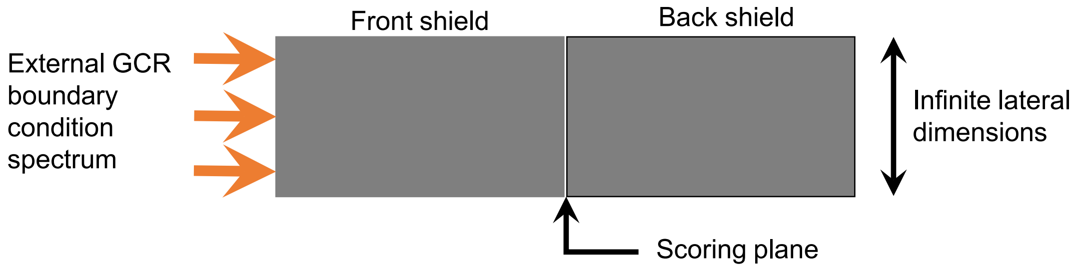

Comparison of HZETRN2020 to Geant4 for 60 g/cm^2 aluminum shielding using the proton component of the November 16-25, 2013 LEO (51.6° inclination, 450 km) GCR environment as a boundary condition.

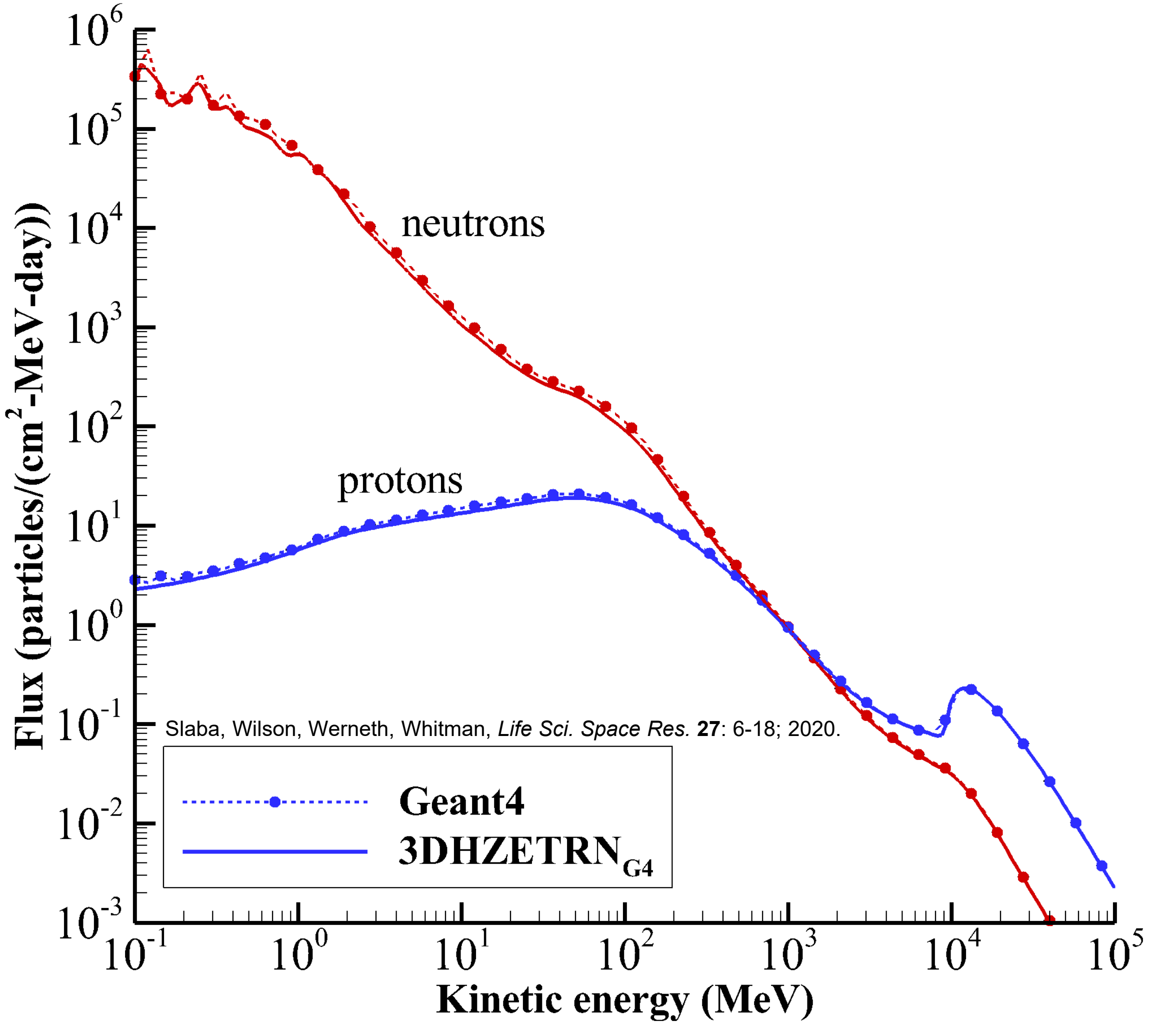

Validation

- **Combined models in good agreement with ISS and BioSentinel measurements**
  - Combined models → GCR, geometry, transport, nuclear physics and magnetic field model for low Earth orbit ISS trajectory
  - Larger errors seen along portions of ISS flight path where absorbed dose is small
  - Moderate compensating errors between underlying models in some cases

ISS geometry analyzed by HZETRN2020. Top: fully detailed CAD model. Bottom: Interpreted geometry from ray-trace information.

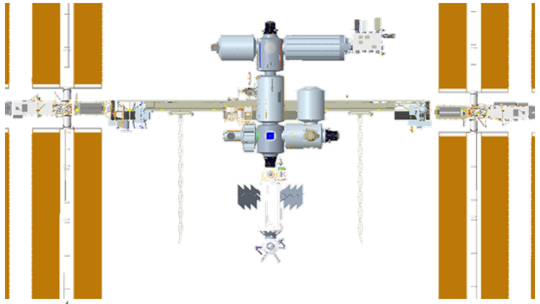

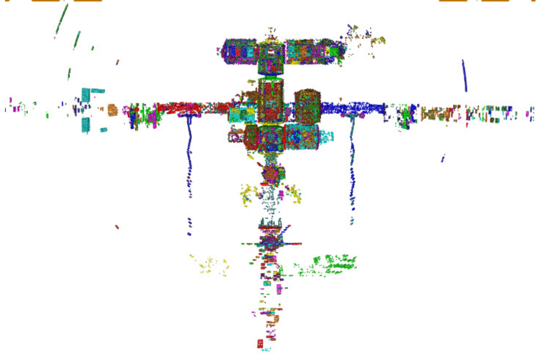

Comparison of modeled and measured absorbed dose in silicon (mGy/day). ISS comparison is for November 16-25, 2013 in the US lab. BioSentinel comparison is for November 16, 2022 – May 16, 2023.

	ISS	BioSentinel
Measurement	0.108	0.247
HZETRN2020	0.106	0.250
Error	(-1%)	(1%)

ISS: Slaba, Wilson, Werneth, Whitman, *Life Sci. Space Res.* **27**: 6-18; 2020.
BioSentinel: Rahmanian, Slaba, Braby, Santa Maria, Bhattacharya, Straume, *Life Sci. Space Res.* **38**: 19-28; 2023.

BioSentinel geometry analyzed by HZETRN2020. Top: fully detailed CAD model. Bottom: Combinatorial geometry.

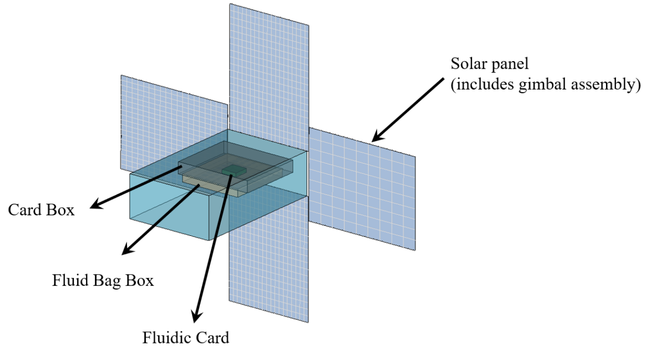

Validation

- **Combined models in good agreement with dose-rate measurements on the surface of Mars**
  - Combined models → GCR, transport, nuclear physics, Mars atmosphere model

Comparison of HZETRN2020 to MSLRAD data.

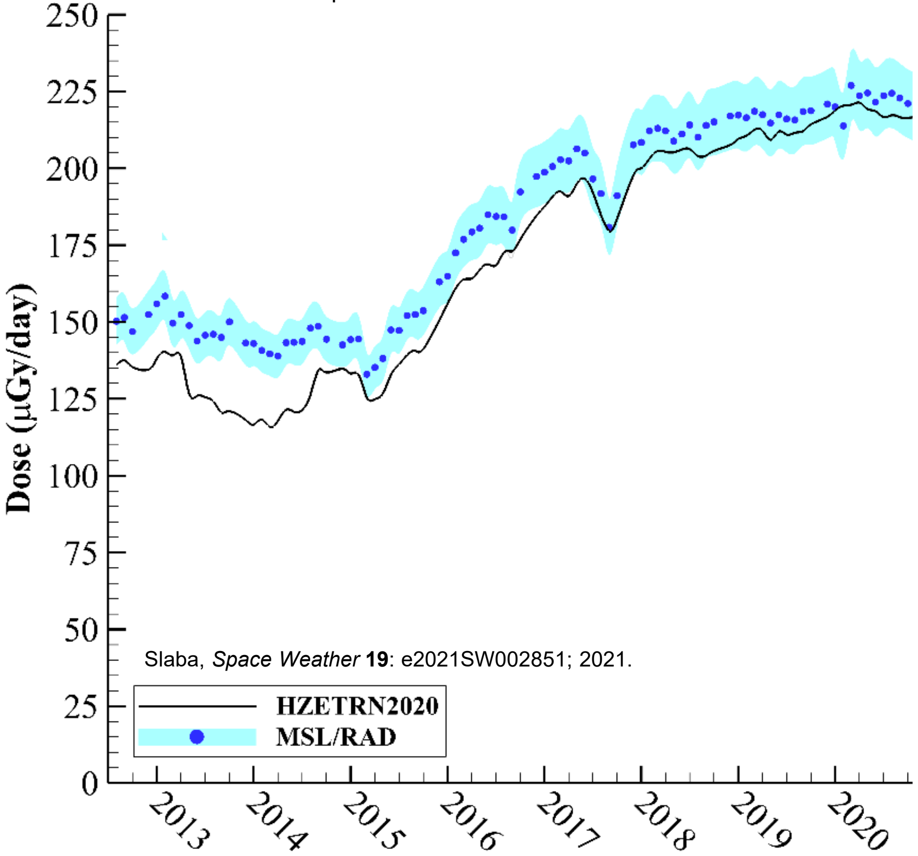

- Average error: 7%
- Bounding errors: -19% and 3%
- Errors during ~2014 solar maximum attributed to GCR model

MSL/RAD – Mars Science Laboratory Radiation Assessment Detector

Space Radiation Overview

- **<u>How</u>** → Space radiation exposures and risks are estimated using integrated models and data

Space radiation environment

nasa.gov/sites/default/files/14-271.jpg

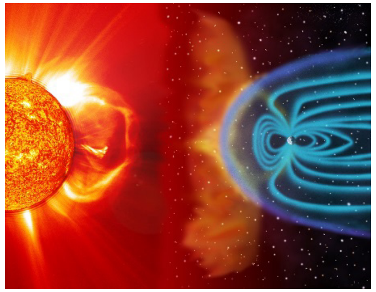

→

Intravehicular radiation field

Simonsen, Slaba, Guida, Rusek, *Plos Bio* **18**: e3000669; 2020.

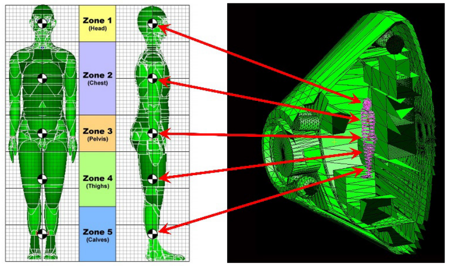

→

Health risk projections

Simonsen, Slaba, Guida, Rusek, *Plos Bio* **18**: e3000669; 2020.

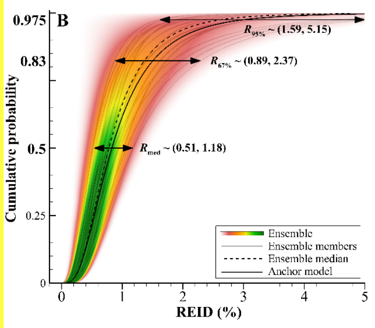

NASA Cancer Risk Model

Projecting space radiation risks from available terrestrial data

Excess risk coefficients
- acute gamma exposure risks
- transferred to target population

Scaled by

Dose and dose-rate effectiveness factor (DDREF)
- scale from acute to chronic exposure

Radiation quality factor
- scale from gamma to mixed ion/energy space radiation

Derived mainly from external epidemiological studies
- Analysis of A-bomb survivors (Life Span Study cohort)
- New data from Million Worker Study (MWS) and International Nuclear Workers Study (INWORKS) being analyzed

Main focus of cancer experimental and modeling efforts
- GCR simulator studies for mixed field and dose-rate effects
- Colorado State University neutron facility for dose-rate effects
- Tumorigenesis and chromosome aberration data and models

Uncertainties *currently* quantified in risk projections

Multiple uncertainties *not yet* quantified in risk projections

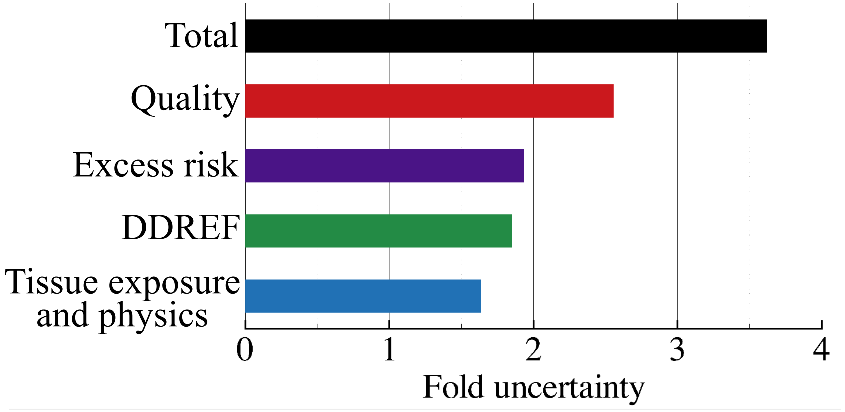

Further reading

- NASA model
  - Cucinotta, Kim, Chappell, NASA TP 2013-207375; 2013.
- Current NASA model within ensemble framework
  - Simonsen, Slaba, *Life Sci. Space Res.* **31**: 14-28; 2021.

Simulations to Inform Quality and Dose-Rate

Track structure visualization from RITRACKS for 25 MeV/n carbon ions

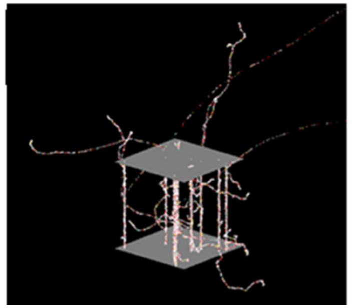

- GCR ions deposit energy to sensitive biological along localized tracks
  - Low energy electrons (δ-rays) are liberated from the target
  - Monte Carlo simulation required to transport δ-rays and study energy deposition at micron scale

- NASA has developed a simulation code to study track-structure effects
  - Developed with GCR induced biological outcomes in mind
  - Includes radiation chemistry along with physics of δ-ray transport
  - Plante, Cucinotta, Book chapter, In Tech: Rijeka, Croatia; 2011.

- Applications of RITRACKS
  - ❖ Coupled to chromosome aberration model RITCARD
    - Plante, Ponomarev, Patel, Slaba, Hada, *Rad. Res.* **192**: 282-298; 2019.
  - ❖ Multi-scale simulations with Geant4
    - Slaba, Plante, Ponomarev, Patel, Hada, *Rad. Res.* **194**: 246-258; 2020.
  - ❖ Ongoing study of nuclear target geometry effects
    - Poignant, Plante, Patel, Huff, Slaba, Int. J. Mol. Sci. **23**: 8636; 2022.
  - ❖ Informing microdosimetric dose-response models form multiple biological endpoints of interest to cancer risk assessment

Comparison of model to experiment for chromosome aberrations (simple exchanges) for 300 MeV/n Ti incident on human fibroblast cells

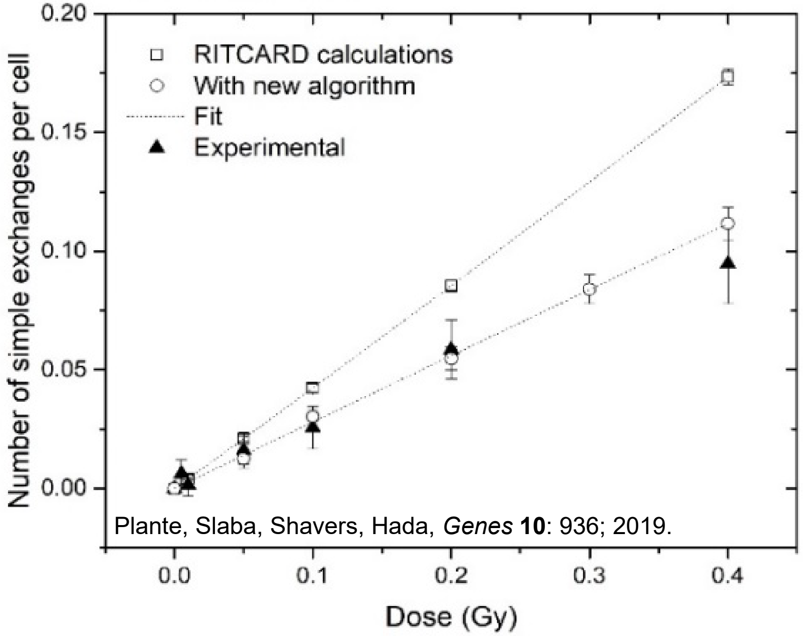

Projections for Deep Space Missions

https://www.nasa.gov/sites/default/files/atoms/files/america_to_the_moon_2024_artemis_20190523.pdf

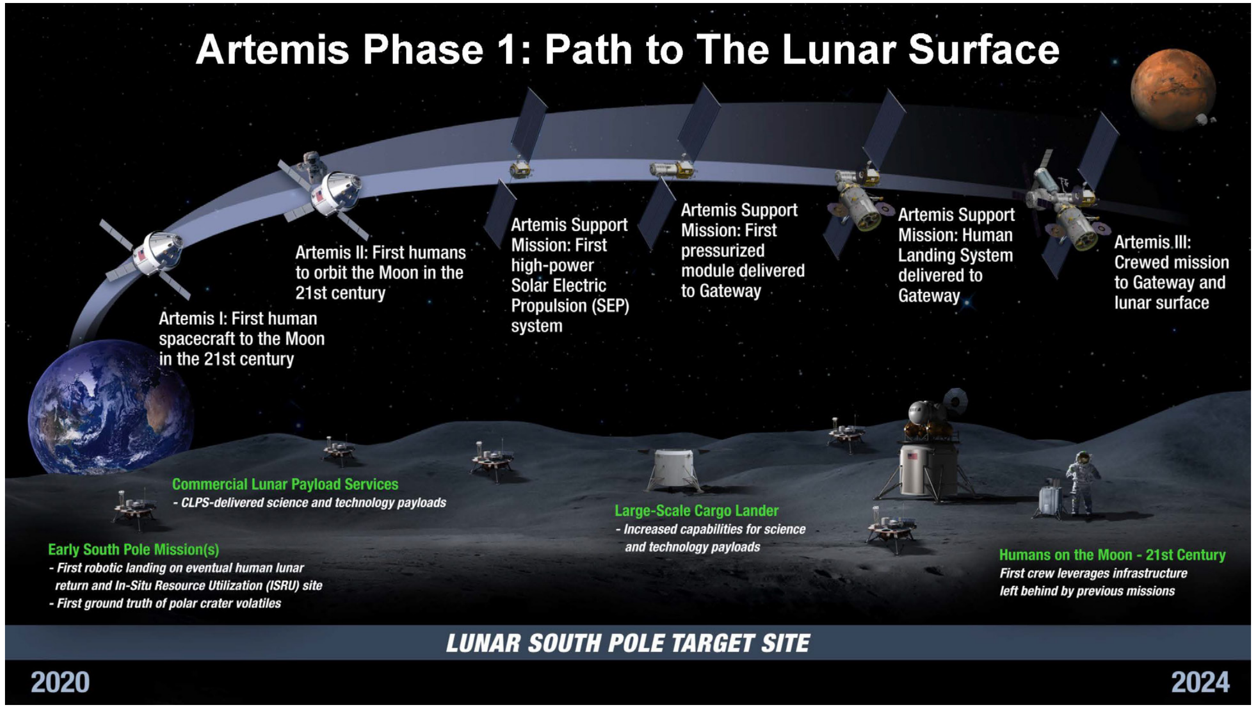

Summary of astronaut mission exposures prior to 2008.

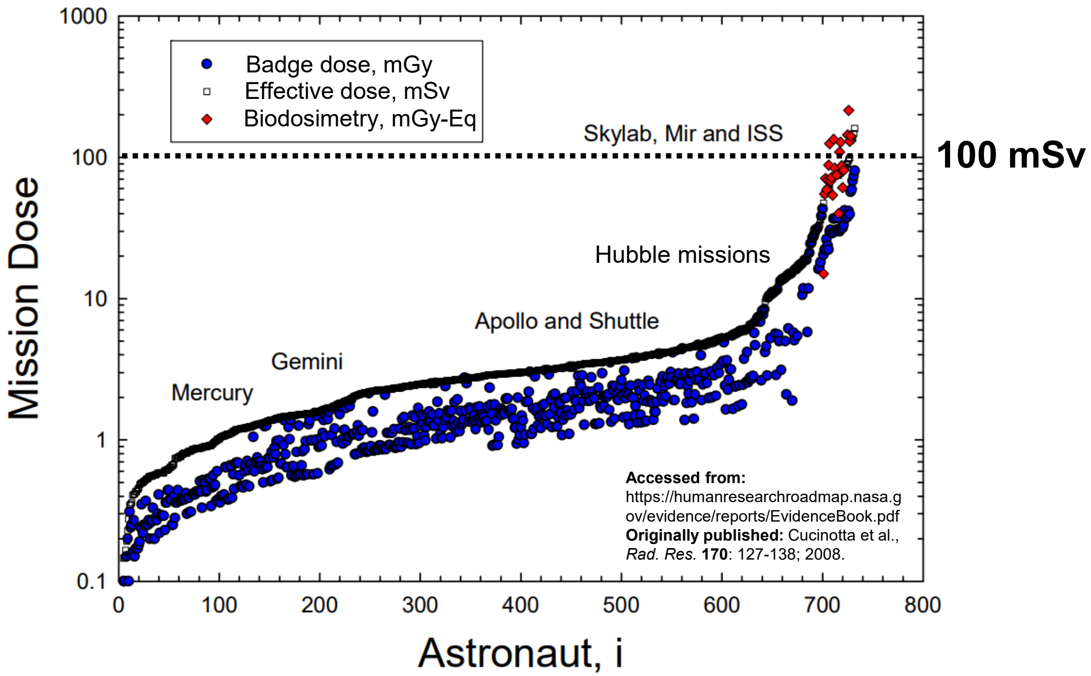

	Artemis II	Artemis III surface ops	Artemis III	6 months Gateway	12 months Gateway	Mars DRM
Duration (days)	10	23.5 + 6.5 surface	30	183	365	621 + 40 surface
Effective dose (mSv)	**10**	**27**	**30**	**182**	**364**	**640**

DRM – Design Reference Mission

Projections for Deep Space Missions

Wide range of upper 95% confidence level (CL) ensemble values

- Equally plausible models give divergent results at high CL
- Traces back to lack of data to constrain underlying models

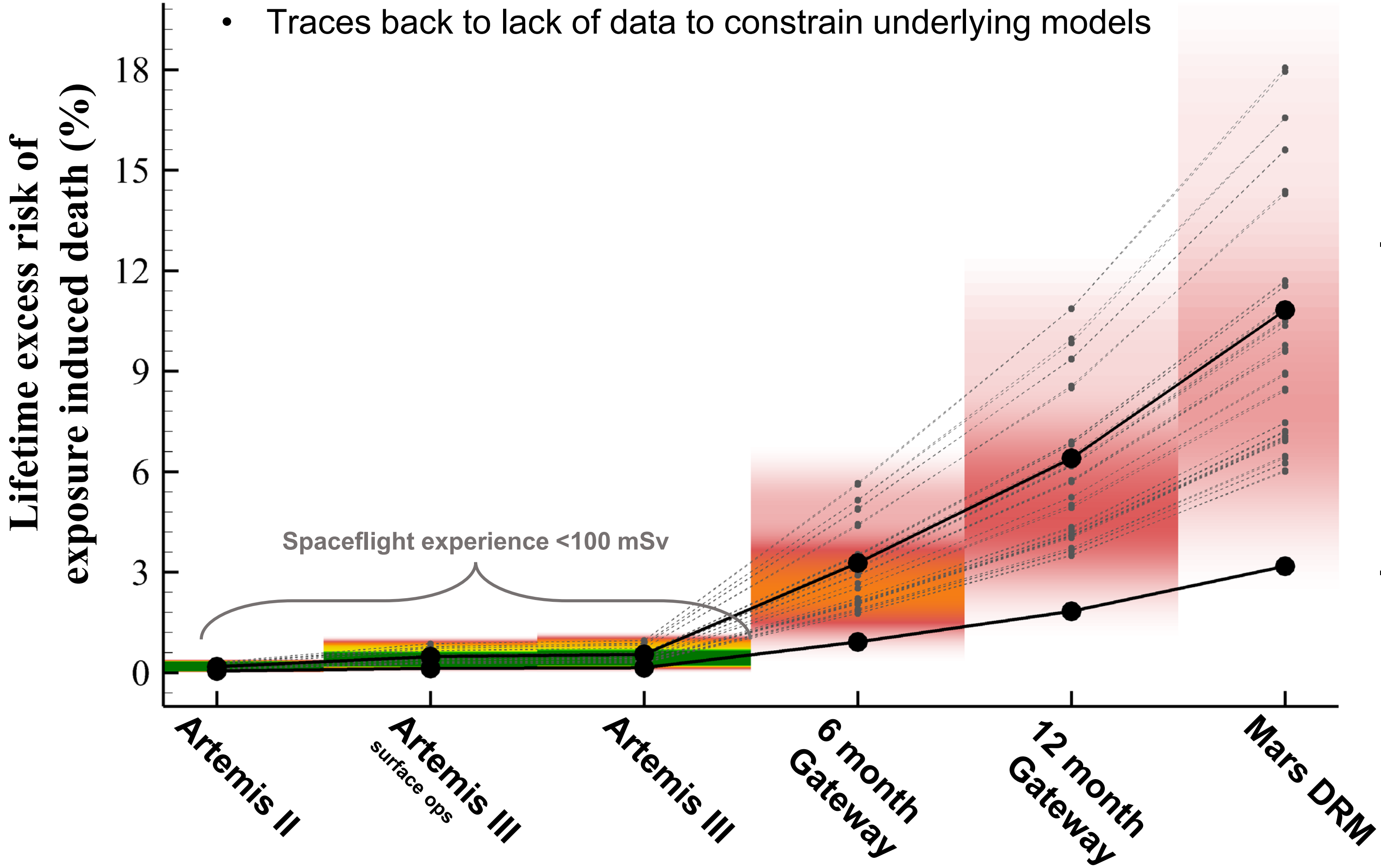

Upper 95% CL risk from all ensemble members with kernel density estimate of ensemble distribution

MEDIAN risk from NASA model

Effective dose (mSv)	10	27	30	182	364	640

Summary

- Radiation exposure is one of the main hazards for human spaceflight
  - Space radiation environment is characteristically different than anything on Earth
  - Need to accurately describe the radiation fields encountered by astronauts to project health risks

- Radiation transport plays a key role in multiple applications
  - Propagating cosmic rays to the vicinity of Earth in GCR models
  - Radiation transport through shielding and tissue
  - Track structure simulations

- Outstanding space radiation transport challenges
  - Application of Monte Carlo simulation to fully detailed vehicle geometry and GCR (has never been accomplished)
  - Track-structure simulations are computationally expensive, making them difficult to incorporate with other biological models
  - Uncertainties in nuclear interaction (cross section) models that underly all transport codes

- Risk-to-dose relationships for future missions (>100 mSv) remain uncertain
  - Exposures are beyond spaceflight experience (lifetime astronaut surveillance provides limited information)
  - Epidemiological models may be improved with large-scale radiation worker studies
  - Ground-based radiobiology data needed to reduce uncertainties for radiation quality and dose-rate effects
  - Several "unknown“ uncertainties remain – individual susceptibility, multiple stressors, animal/human translation